also some of the crystalline part (probably surrounding regions of the crystalline part) of PVF$_2$. And the fraction of PMeOZO is limited constructing a miscible phase in the PMeOZO-PVF$_2$ blend (<50%).

Conclusion. PMeOZO-PVC and PMeOZO-PVF$_2$ blends are miscible in the blend fraction range of PMeOZO lower than 50 wt %. PPrOZO is miscible with PSt in the range of the PPrOZO fraction lower than 25 wt %. Both PMeOZO-PP and PEtOZO-PP blends are not miscible. These results provide fundamental, important data when new polymer materials are desired from blends of these polymers and/or copolymers.

Acknowledgment. We are indebted to the Ministry of Education, Science and Culture, Japan, for partial support by Grant-in-Aid for Environmental Science (Nos. 58030001 and 59030003). We acknowledge Dr. A. Tanaka (Kyoto University) for rheovibron measurements and for his constant advice and Drs. M. Shimbo and M. Ochi (Kansai University) for their help in performing torsional braid analysis. We also express our appreciation to Drs. H. Kusanagi and M. Kashima (Unitika Co.) for wide-angle X-ray and DSC measurements.

Registry No. PVC, 9002-86-2; PSt, 9003-53-6; PP, 9003-07-0; PVF$_2$, 24937-79-9; PMeOZO (homopolymer), 26375-28-0; PMeOZO (SRU), 25805-17-8; PEtOZO (homopolymer), 25822-74-6; PEtOZO (SRU), 38796-76-8; PPrOZO (homopolymer), 69488-61-5; PPrOZO (SRU), 25821-74-3.

References and Notes

(1) Olabisi, O.; Robeson, L. M.; Shaw, M. T. *Polymer-Polymer Miscibility*; Academic: New York, 1979.
(2) Paul, D. R., Newman, S., Ed. *Polymer Blends*; Academic: New York, 1979.
(3) Paul, D. R.; Barlow, J. W. *J. Macromol. Sci., Rev. Macromol. Chem.* **1980**, *6*, 109.
(4) Matzner, M.; Robeson, L. M.; Wise, E. W.; McGrath, J. E. *Makromol. Chem.* **1982**, *183*, 2871.
(5) Paul, D. R.; Altamirano, J. O. *Polym. Prepr. (Am. Chem. Soc., Div. Polym. Chem.)* **1974**, *15*, 409.
(6) Nishi, T.; Wang, T. T. *Macromolecules* **1975**, *8*, 909.
(7) Hourston, D. J.; Hughes, I. D. *Polymer* **1977**, *18*, 1175.
(8) Boerdink, E.; Challa, G. *Polymer* **1978**, *19*, 173.
(9) Keskkula, H.; Paul, D. R. *J. Appl. Polym. Sci.* **1986**, *31*, 1189.
(10) Kobayashi, S.; Kaku, M.; Saegusa, T. *Polym. Prepr. Jpn.* **1983**, *32*, 1403; **1984**, *33*, 2775.
(11) Kobayashi, S.; Saegusa, T. *Makromol. Chem. Suppl.* **1985**, *12*, 11.
(12) Kobayashi, S.; Kaku, M.; Saegusa, T., unpublished results.
(13) Bassiri, T. G.; Levy, A.; Litt, M. *Polym. Lett.* **1967**, *5*, 871.
(14) Takayanagi, M.; Hirama, H.; Iwata, Y. *Memory Faculty Engineering Kyushu Univ.* **1963**, *23*, 1.
(15) Yano, L. *J. Polym. Sci., Polym. Phys. Ed.* **1970**, *8*, 1057.
(16) Osaki, S.; Ishida, Y. *J. Polym. Sci., Polym. Phys. Ed.* **1974**, *12*, 1727.
(17) Imken, R. L.; Paul, D. R.; Barlow, J. W. *Polym. Eng. Sci.* **1976**, *16*, 593.
(18) Kwei, T. K.; Patterson, G. D.; Wang, T. T. *Macromolecules* **1976**, *9*, 780.
(19) Hasegawa, R.; Takahashi, Y.; Chatani, T.; Tadokoro, H. *Polym. J.* **1972**, *3*, 600.
(20) Lando, J. B.; Olf, H. G.; Apeterlin, A. *J. Polym. Sci. Polym. Chem. Ed.* **1966**, *4*, 941.

Molecular Motions in Model Network Polymers

L. Charles Dickinson, P. Morganelli, C. W. Chu, Z. Petrović, William J. MacKnight, and James C. W. Chien*

Department of Polymer Science and Engineering, University of Massachusetts, Amherst, Massachusetts 01003. *Received January 13, 1987*

ABSTRACT: Molecular motions in network polymers of monodisperse PPO, α,ω-dihydroxypoly(propylene oxide), cross-linked with TIPTP, tris(4-isocyanatophenyl) thiophosphate, were compared with those of linear polymers of the same molecular weight PPO chains extended with diisocyanates. The linear polyurethanes have a single exponential decay for $T_{1\rho}$(C) with well-defined $T_{1\rho}$(C) minima that occur at lower temperatures for longer PPO segments. Samples of 1000 MW PPO chains extended with phenylene-1,4-diisocyanate show the same $T_{1\rho}$(C) values by cross polarization or direct polarization while these values are different for toluene-2,4-diisocyanate linked polymers, indicating the presence of regions of dissimilar rigidity. The decay of backbone carbon magnetization is biphasic for networks with PPO MW 400–2000. The fast components have values very close to the corresponding $T_{1\rho}$(C) value for the aromatic carbons. The former is probably the relaxation of those backbone atoms in proximity with and closely coupled to the phenyl group of TIPIP while the slow component is associated with the remote backbone carbons. The networks formed from MW 3000 PPO have $T_{1\rho}$(C) behavior resembling that for the linear polyurethanes according to both cross and direct polarization. CP-MAS-^{13}C NMR thus yields a biphasic decay for networks with short interconnecting chains, but when the length of chains approaches 3000, the relaxation becomes simple exponential and closely resembles that of linear chain systems.

Cross-linked polymeric systems span a wide range of properties and applications from swollen gels of hydroxyethyl methacrylates to rubbers, engineering resins, and composite matrix materials. Physicochemical measurements on these systems are naturally limited to those which do not require their dissolution. Most of the techniques measure the macroscopic properties. Any new method that can reveal details of the molecular motion and indeed any discrimination of regions within a network would contribute toward further advances in the basic understanding and designing of new network systems.

There is extensive literature on nuclear magnetic relaxation in polymeric networks and rubbery materials. Early work relied upon the decrease with temperature of the second moment of the featureless proton line shape to detect component motions and could distinguish segmental and methyl motion in favorable cases, such as polypropylene, polyisobutylene, and natural rubber.[1] Spin-lattice relaxation times of the protons, T_1(H), could be measured to differentiate between the same motions in poly(isobutylene).[2] Spin-lattice relaxation in the rotating frame, $T_{1\rho}$(H), was found to be a useful parameter in mapping low-frequency motions (tens of kHz) in polymers[3] including poly(propylene oxide).[4] The subject of NMR in solid polymers has been reviewed.[5,6] Several studies are of special relevance to our work. In particular

0024-9297/88/2221-0338$01.50/0

a study of T_1(H) in poly(*cis*-butadiene) randomly cross-linked with peroxide has shown a decrease in T_1(H) at temperatures above the T_1 minimum that was interpreted as indicative of a broad distribution of correlation times near the cross-link.[7] An extension of that work examined T_1(H), $T_{1\rho}$(H), and T_2(H) at several frequencies. T_2(H) varied markedly with M_c, molecular weight between cross-links.[8] Other studies of radiation cross-linked poly(*cis*-isoprene) and of poly(dimethylsiloxane)[10] and their gels emphasized the separate observability of entanglements and cross-links via their T_2(H) dependences upon molecular weight.

With the advent of spectrometer improvements ^{13}C spectra of polymeric systems were analyzed to obtain the distribution of correlation times.[11] Addition of rapid sample spinning at the magic angle allowed examination of vulcanized or filled polymeric systems.[12]

To limit the importance of the variable of distribution of MW between cross-links, we have undertaken a study of model network polymers derived from narrow distribution PPO and a triisocyanate, TIPTP. Linear counterparts were obtained by chain extending these PPO's with diisocyanates. Comparisons of these two types of systems showed the effect of cross-linking on the molecular motion. Emphasis was placed on measurements at temperatures above and below T_g. $T_{1\rho}$(C) and $T_{1\rho}$(H) at resolved resonances were determined. The central purpose of this work is to extend the previous studies to exploit more fully the potentials of magic angle spinning with cross polarization (MAS-CP-NMR) in gaining basic knowledge about molecular motions in network polymers.

Experimental Section

Material. α,ω-Dihydroxypoly(propylene oxide), PPO, of nominal molecular weight 425, 1000, 2000, 3000, and 4000 was obtained from Aldrich Chemical. By gel permeation chromatography and vapor pressure osmometry the PPO's were found to have the following molecular weights (polydispersities), respectively: 454 (1.01); 965 (1.01); 2020 (1.01); 3000 (1.03). They all titrated to an OH functionality of 2.00 ± 0.15. The PPO was azeotropically dried in dry benzene and stored under dry nitrogen or in vacuo. Tris(4-isocyanatophenyl) thiophosphate, TIPTP (Mobay Chemicals), was recrystallized twice from toluene at −20 °C. Dibutylamine titration showed the TIPTP to contain ≥98% of the required isocyanate functionality.

Networks were prepared by dissolving under dry nitrogen $^1/_3$ mol of TIPTP with $^1/_2$ mol of PPO, heating to 90 °C in a vacuum oven for 12–48 h. Infrared spectroscopy showed no remaining isocyanate absorptions. Network systems prepared from 425, 1000, 2000, 3000, and 4000 MW PPO are designated as N(0.4K), N(1K), N(2K), N(3K), and N(4K), respectively.

Linear polyurethanes were also prepared by chain extension of PPO either with toluene-2,4-diisocyanate with designations L(*n*K)2,4 or with *p*-phenyl diisocyanate designated as L(*n*K)1,4 where *n*K corresponds to MW of PPO and L distinguishes linear from network systems. The chain extension reaction conditions are the same as those given above for network formation. By GPC the following $\bar{M}_w$ and polydispersisities were determined: L(1K)2,4, 103 000, 2.89; L(3K)2,4, 60 800, 2.8; L(1K)1,4, 160 000, 1.6.

Method. An IBM 200 AF spectrometer with solids accessory was used in this study with ^{13}C observed at 50.3 MHz. The polymer samples were ground to 100-μm size powder in a Spex Freezer Mill (Spex Industries, Edison, NJ) which facilitates uniform packing in a rotor in order to be spun at 5 kHz. Recycle time was generally 3 s, and FID's were summed. For cross-polarization (CP) sequences, a 5 μs $\pi/2$ proton pulse was followed by a simultaneous Hartmann–Hahn spin locking of ^{13}C and ^{1}H for 0.5–2 ms depending upon the sample and temperature. With the ^{1}H field turned off the ^{13}C spin lock was maintained for a time, τ, after which ^{13}C magnetization was monitored with ^{1}H decoupling. For the direct polarization (DP) experiment, a 5 μs $\pi/2$ ^{13}C pulse was followed by ^{13}C spin locking for time τ followed by decoupling during the receiver-on period. $T_{1\rho}$(H) was obtained by spin-locking protons for a time τ prior to the cross polarization. Relaxation times were obtained as slopes of semilog plots of ^{13}C intensity versus τ. Variable temperature was controlled by a Bruker control unit with accuracy of ±1 °C.

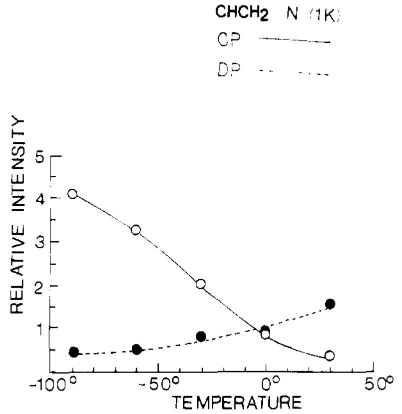

Figure 1. Relative intensity of the backbone carbon resonances in N(1K) samples as a function of temperature by (○) cross polarization and (●) direct polarization.

Dynamic mechanical measurements were obtained at 10 Hz on a DMTA; dielectric loss was measured at 1 KHz on a DETA. Both instruments are manufactured by Polymer Laboratories (Amherst, MA).

Results

Magnetization by Direct and Cross Polarizations. There is an intrinsic limitation to the MAS-CP-NMR technique in obtaining data over a wide range of temperatures for noncrystalline substances. This is illustrated in Figure 1 for the N(1K) network. At low temperatures CP is efficient, but as temperature increases, the dipole–dipole interaction responsible for polarization transfer becomes progressively weaker as segmental motion increases with temperature. In the high-temperature limit CP should vanish since the dipolar tensor has zero trace. Signal intensity for CP sequences can thus drop by an order of magnitude or more over the −90 to +50 °C range examined (Figure 1). Fortunately, DP is not affected in the same way and the polymers give strong signals above T_g with simple DP by $\pi/2$ pulses. On the other hand, as the temperature is lowered, the DP signal weakens. Presumably as motional freedom decreases T_1(C) lengthens, the time of delay between pulses was probably insufficient for the return of spin to equilibrium. Some experiments with recycle delays of 10, 20, and 30 s for the DP experiment showed an increase in intensity corresponding to an approximate T_1(C) of 100 s. ^{13}C relaxation in the rotating frame is a complicated process; in fact, the $T_{1\rho}$(C) values found by DP and CP magnetization are not always in agreement. In principle if DP and CP detected the same rigid ensemble of carbon nuclei, the latter would be 4 times as intense as the former. This condition is evidently not true for the backbone carbons of the N(1K) sample (Figure 1), suggesting that there are regions of differing rigidity which are preferentially sampled by the CP and DP measurements.

Variation of cross polarization time for our networks below T_g gives the typical T_{CH} rise in ^{13}C intensity with $T_{1\rho}$(H) decline at longer CP times. The maximum intensity occurs in 0.5 ms for N(3K) and 2.0 ms for N(0.4K) materials. Near T_g the ^{13}C intensity drops precipitously, but the CP intensity versus CP time curve retains the same shape. Above T_g the ^{13}C intensity shows a linear increase with τ_{CP} with no maximum observed that is typical for cross polarization of rubbery materials.

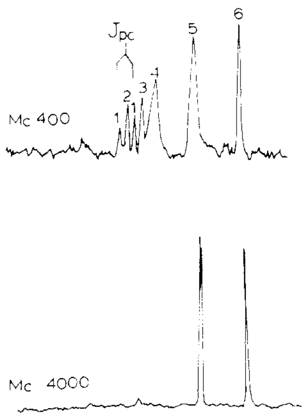

Figure 2. MAS-CP-^{13}C NMR spectra of (a) N(0.4K) and (b) N(4K) samples at room temperature. Peak assignments are 1, P–O–C_{arom}; 2, C=O; 3, C_{arom}–N; 4, C_{arom}H; 5, –CHCH$_2$–; 6, CH$_3$.

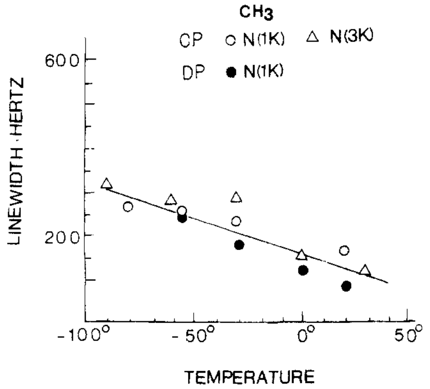

Figure 3. Methyl carbon resonance line width as a function of temperature for N(1K) sample (○) by CP and (●) by DP and for N(3K) sample (△) by CP.

Line Width. The CP-NMR spectra of N(0.4K) and N(4K) are shown in Figure 2; the former have considerably broader lines than the latter. The two backbone carbon resonances are unresolved in the lower MW networks but are partially resolved in the high MW network specimen. The protonated and unprotonated aromatic resonances of TIPTP are evident. As the molecular weight between cross-links is increased, the aromatic resonances diminish in relative intensity.

The variation of line width with temperature for N(1K) and N(3K) samples has been studied. For the methyl resonance (Figure 3), there is a monotonic decrease of line width with increase of temperature as observed by either CP or DP. The backbone carbons have broader line widths than the methyl carbons (Figure 4). For the N(1K) samples the line width is unchanged with increasing temperature, but above −10 °C it decreases rapidly. Samples with longer PPO chains (and thus lower T_g) have line widths that begin to decrease at a lower temperature as illustrated for the N(3K) sample in this figure.

For the linear polyurethane the CH$_3$ carbon line width exhibits the same temperature variation as the network systems (Figure 5). However, the line width of the backbone carbons is practically temperature-independent.

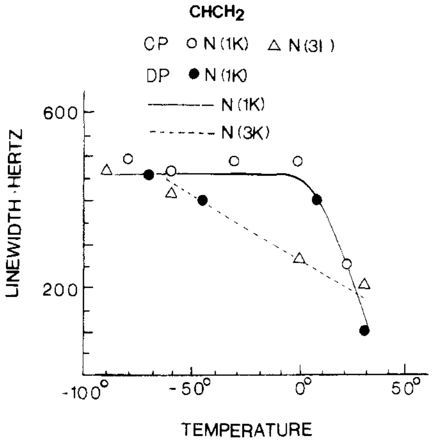

Figure 4. Backbone carbon resonance line width as a function of temperature for N(1K) sample (○) by CP and (●) by DP and for N(3K) sample (△) by CP.

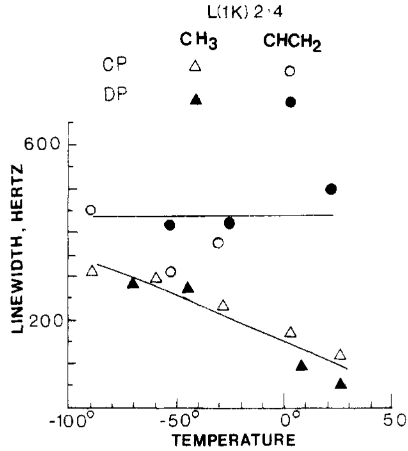

Figure 5. Carbon resonance line width as a function of temperature: (○) backbone carbons by CP, (●) backbone carbons by DP, (△) methyl carbons by CP, (▲) methyl carbons by DP.

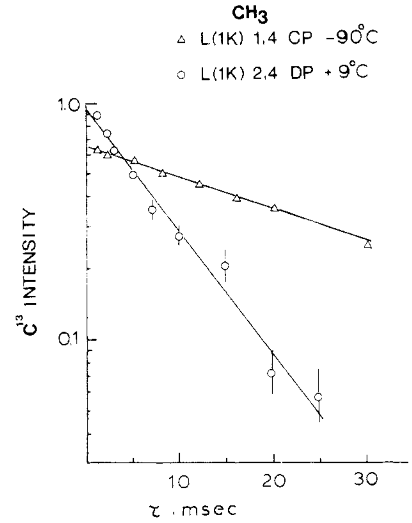

Figure 6. Variation of ^{13}C intensity versus delay time of cross polarization: (△) L(1K)1,4, −90 °C; (○) L(1K)2,4, +9 °C.

Spin–Lattice Relaxation of Carbon in Linear Polyurethanes. The semilog plots of ^{13}C NMR intensity versus spin lock time are characterized by a single exponential decay (Figure 6). Values of $T_{1\rho}$(C) are then simply calculated from the slope. The variation of $T_{1\rho}$(C) versus temperature for the L(1K)1,4 polymer is plotted in Figure 7. The backbone $T_{1\rho}$(C) has a minimum at 0° with a value of 0.5 ± 0.1 ms, corresponding to $\omega_0\tau_c = 0.5$. Since $\omega_0 =$ 50 kHz, $\tau_c = 10$ μs near 0 °C. $T_{1\rho}$(C) increases monotonically on both sides of the minimum. The slope is somewhat smaller at the low-temperature side of the minimum. The same results are obtained with CP or DP. CP sensitivity is poor above room temperature. The methyl $T_{1\rho}$(C) minimum of ca. 5 ms was found near −10 °C. The differences in minimum position show that at a given temperature the CH$_3$ carbon has a shorter correlation time. In fact, by shifting Figure 7b vertically down by 5 ms and

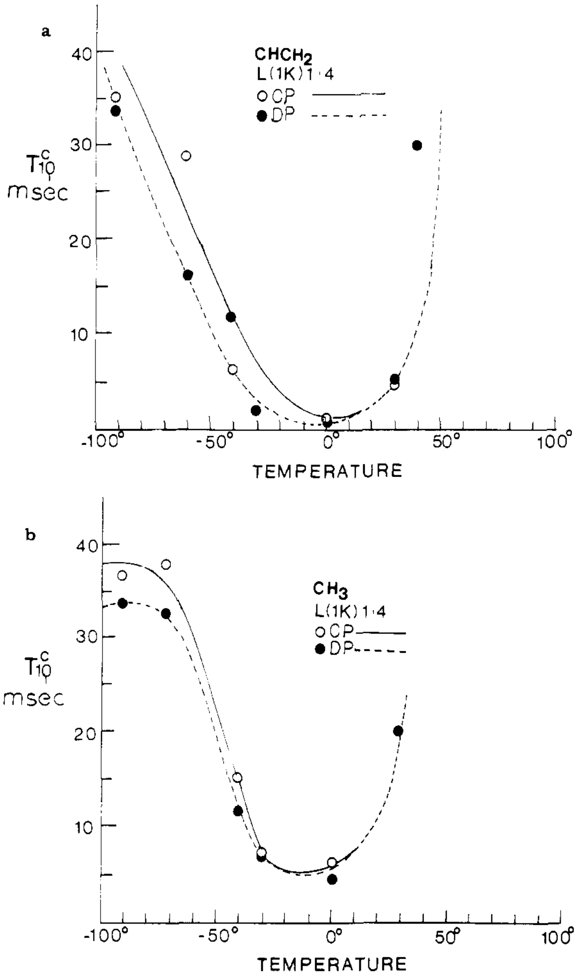

Figure 7. Variation of $T_{1\rho}$(C) of L(1K)1,4 sample as a function of temperature by (○) CP and (●) DP: (a) backbone carbons; (b) methyl carbons.

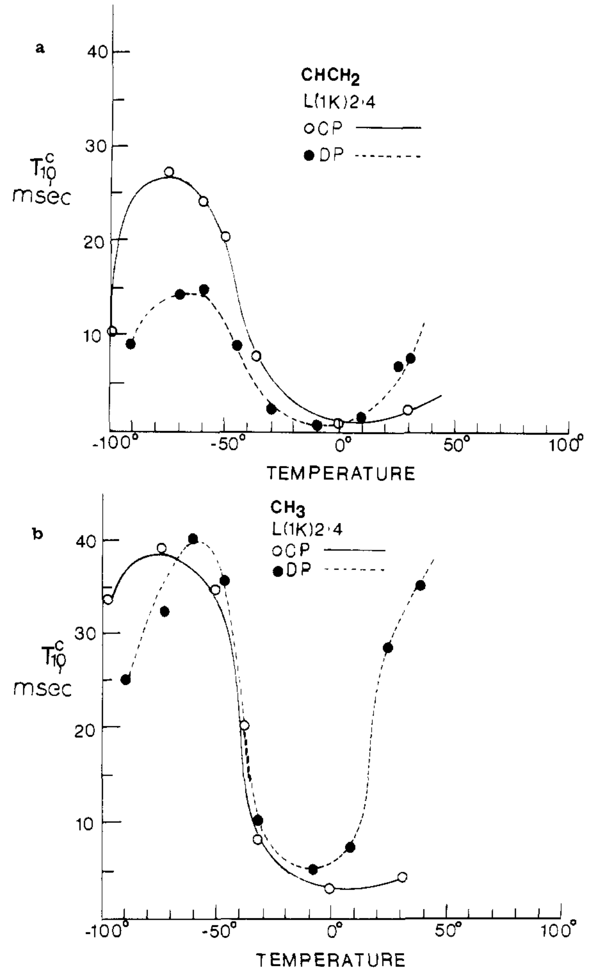

Figure 8. Variation of $T_{1\rho}$(C) of L(1K)2,4 sample as a function of temperature by (○) CP and (●) DP: (a) backbone carbons; (b) methyl carbons.

horizontally by +12 °C the curve can be brought into superposition with Figure 7a. At the low-temperature limit of our spectrometer the $T_{1\rho}$(C) values for the methyl resonance appears to reach a plateau. In this region $T_{1\rho}$(C) is a bit larger by CP than by DP. In general, the $T_{1\rho}$(C) versus temperature dependence is appreciably narrower for the methyl carbon than it is for the backbone carbons, suggesting a broader distribution of molecular motions affecting the relation of the backbone carbons.

Chain extension with toluene-2,4-diisocyanate noticeably alters the details of relaxation behavior as shown in Figure 8. Though their $T_{1\rho}$(C) values at the minima are comparable to the corresponding values for the L(1K)1,4 polymer, the minima for the two resonances are now observed at the same temperature of −7 °C. For temperatures higher than the $T_{1\rho}$(C) minimum the values obtained by CP only increase slightly with temperature so that they are shorter than those found with DP. This is true for both the backbone and methyl carbons. Below the minimum $T_{1\rho}$(C) at first increases with decreasing temperature but goes through a maximum. For the backbone carbons (Figure 8a) the maxima occur at −74 and −64 °C for CP and DP, respectively. The CP relaxation times are always longer. The maxima for the $T_{1\rho}$(C) for methyl carbon by CP and DP differ by about 20 °C, but $T_{1\rho}$(C) by CP and DP are the same between −50 and −70 °C.

The sensitivity of motion to PPO length between urethane units is shown by results in Figure 9 for L(3K)2,4. It is interesting that the $T_{1\rho}$(C) minimum occurs at −40 °C for both backbone and methyl carbons having the values of 0.5 and 3.5 ms, respectively. The relaxation times are the same for either CP or DP. At elevated temperatures, i.e., 40 °C, $T_{1\rho}$(C) becomes quite long with values of 60 and 175 ms for the backbone and methyl carbons, respectively.

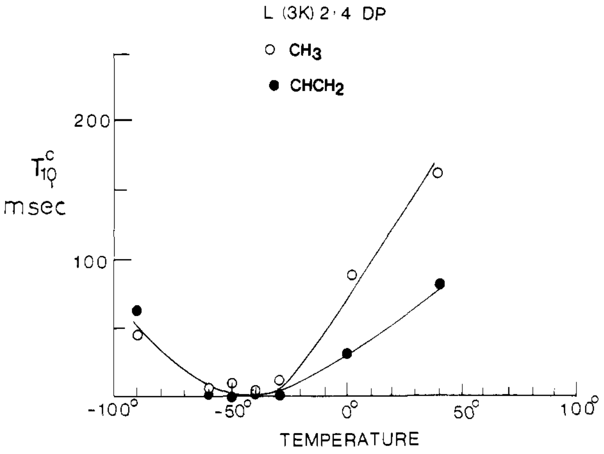

Figure 9. Variation of $T_{1\rho}$(C) of L(3K)2,4 sample as a function of temperature by DP: (○) methyl resonance; (●) backbone resonances.

Spin-Lattice Relaxation of Carbon Nuclei in Network Systems. The most significant differences between the linear and cross-linked polyurethanes are that the N(0.4K), N(1K), and N(2K) have ^{13}C NMR decays which are biphasic whereas the linear and N(3K) samples show a single exponential decay. The biphasic plots are illustrated in Figure 10. At −90 °C the slow decay phase is

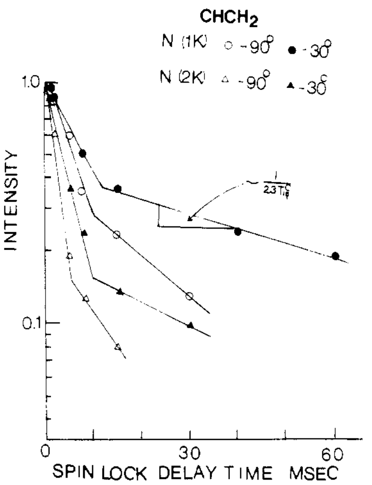

Figure 10. Decay of backbone carbon resonances in the rotating frame with time for the following: (○) N(1K) at -90 °C; (●) N(1K) at -30 °C; (△) N(2K) at -90 °C; (▲) N(2K) at -30 °C.

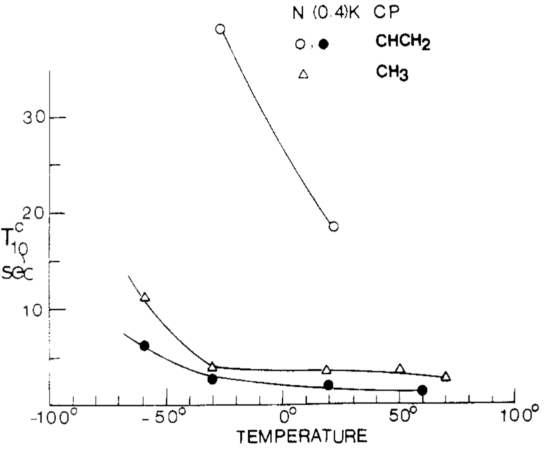

Figure 11. Variation of $T_{1\rho}$(C) versus temperature for N(0.4K) sample: (○, ●) backbone carbons, CP (slow and fast components); (△) methyl carbon, CP.

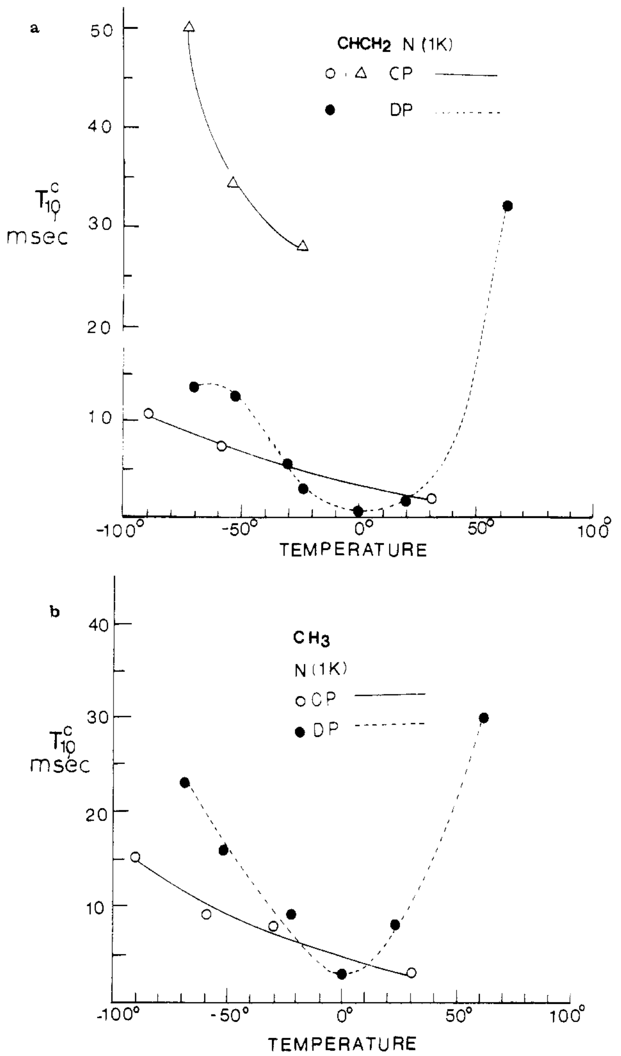

Figure 12. Variation of backbone $T_{1\rho}$(C) versus temperature for N(1K) sample by (○, △) CP (fast and slow component) and (●) DP: (a) backbone carbons; (b) methyl carbons.

about one-half of the total whereas only about 20% of the ^{13}C intensity decays slowly at −30 °C; there is about one-third of a slow component for the N(0.4K) samples at −30 °C. Therefore, both the decay rates and the relative contributions of the two components are dependent upon temperature and M_c. There is little doubt that the slope of the slow decaying process corresponds to the assigned spin–lattice relaxation time. On the other hand there is no basis to analyze the initial decay according to concurrent or consecutive first-order kinetics. Therefore, we just report the apparent $T_{1\rho}$(C) for the first component as obtained from the initial slope. Because of spin diffusion it is well-known that quantitative interpretation of fraction of slope of each component is impossible.

Now we present the data on the network polymers in the order of increasing M_c. The $T_{1\rho}$(C) values for the methyl backbone resonances (Figure 11) by CP for N(0.4K) sample are about twice that for the backbone carbons. The change of relaxation time with temperature is very slight over a broad range of −30 to +70 °C without a distinct minimum. These relaxation times are notably very short. For this material the DP signal is quite weak so accurate relaxation times are difficult to obtain, but a few data points show them to be comparable to the CP results. The low-temperature CP sequences have distinctly biphasic decay for the relaxation of the backbone resonance.

The N(1K) material has the rapid CP decay phase $T_{1\rho}$(C) values comparable to the N(0.4K) samples, and no minimum was observed by CP (Figure 12). On the other hand the DP results showed a definite minimum in the vicinity of 0 °C with $T_{1\rho}(C) = 0.86$ ms for the backbone carbons and 3 ms for the methyl carbons. The $T_{1\rho}$(C) versus temperature plot is almost symmetric for the methyl resonance by DP. Like the N(0.4K) sample, the decay of the CP backbone resonance for N(2K) is biphasic.

The behavior of the relaxation for N(2K) material is like that of the lower M_c samples except in this case the $T_{1\rho}$(C) values for both the backbone and methyl carbons are nearly the same throughout the temperature range investigated (Figure 13).

The N(3K) samples have a relaxation behavior like the L(1K)1,4 chain extended polymer as shown in Figure 14. The $T_{1\rho}$(C) minimum is found that −29 °C with very short $T_{1\rho}$(C) values for the backbone of 0.5 and 0.8 ms by CP and DP, respectively, and corresponding values of 1.5 and 3.0 ms for the methyl resonance. The symmetry of the $T_{1\rho}$(C) versus T plot breaks to low slope at the low-temperature region. It is important to note that the decay obeys simple first-order kinetics.

The relaxation of the protonated aromatic peak at 126 ppm can be followed over the −90 to +60 °C temperature range for the N(0.4K) sample, but only up to T_g for the N(1K) and N(2K) materials (Figure 15). In all these cases $T_{1\rho}$(C) is quite short. A minimum is found at +30 °C, which is near the dielectric and mechanical T_g, for the N(0.4K) systems. In the other polymers there is only a

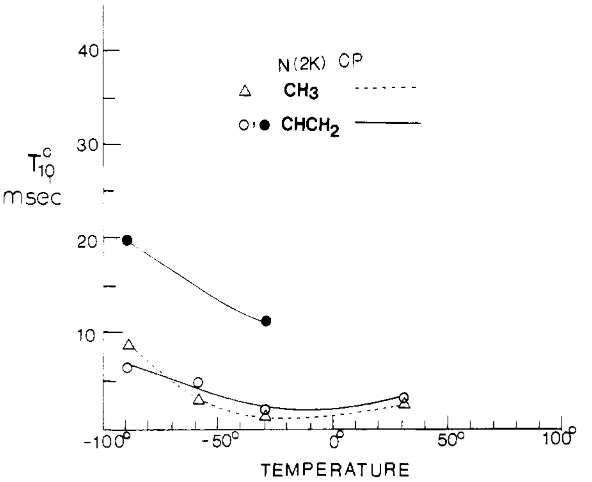

Figure 13. Variation of $T_{1\rho}(C)$ by CP with temperature for N(2K) samples: (○, ●) backbone carbons (fast and slow component); (△) methyl carbon.

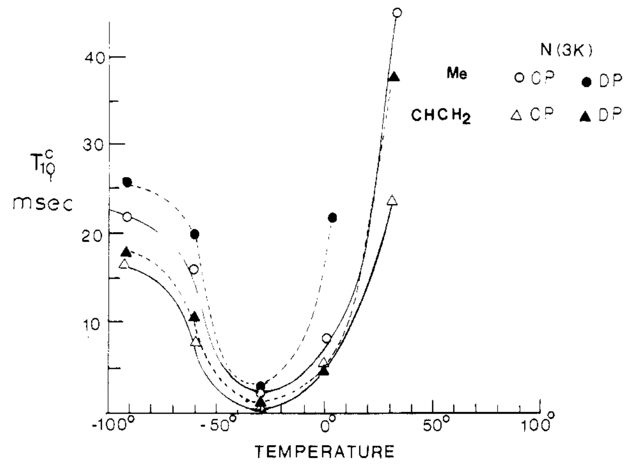

Figure 14. Variation of $T_{1\rho}(C)$ with temperature for N(3K) samples: methyl carbon, (○) CP and (●) DP; backbone carbons, (△) CP and (▲) DP.

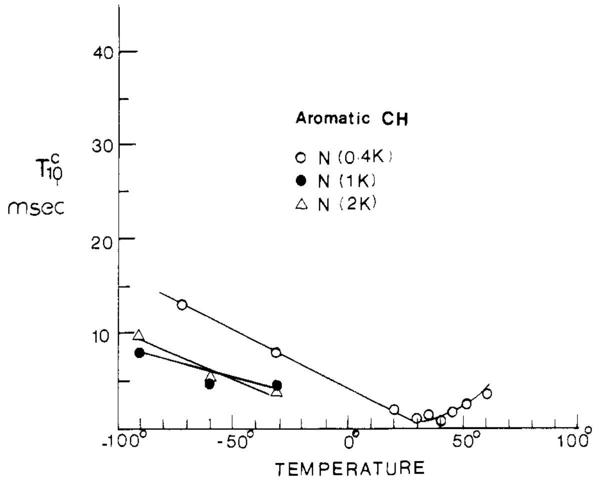

Figure 15. Variation of aromatic carbon $T_{1\rho}$ with temperature for (○) N(0.4K), (●) N(1K), and (△) N(2K).

gradual decrease of relaxation times with temperature increase.

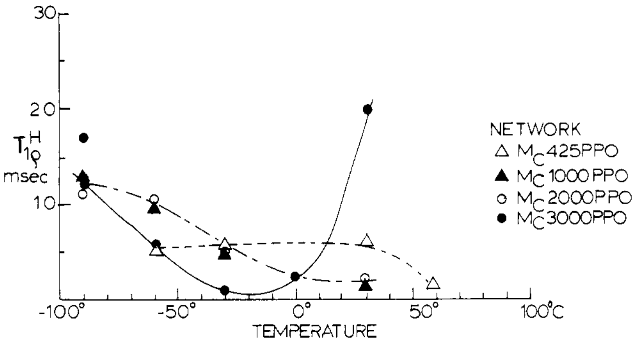

Figure 16. Variation of $T_{1\rho}(H)$ with temperature for (△) N(0.4K), (▲) N(1K), (○) N(2K), and (●) N(3K) networks.

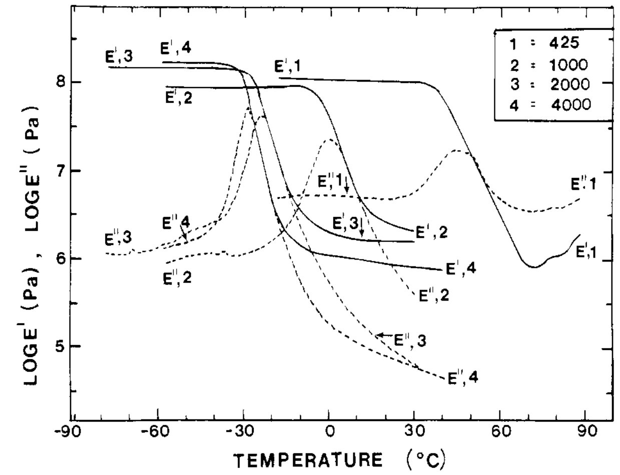

Figure 17. Variation of dynamic (E″) loss and storage (E′) modulus at 10 Hz with temperature for (1) N(0.4K), (2) N(1K), (3) N(2K), and (4) N(4K) networks.

Table I
Temperatures of Mechanical and Dielectric Relaxations

sample	dynamic[a] mechanical (E′ onset)	dielectric[b] (onset)
N(4K)	-45	-60
N(3K)		-50
N(2K)	-40	
N(1K)	-15	-30
N(0.4K)	+30	+20

[a] At 10 Hz. [b] At 1 kHz.

Rotating-frame spin–lattice relaxation of the protons, $T_{1\rho}(H)$, was also measured by a CP technique. In all cases the same $T_{1\rho}(H)$ values were found for the CH_3 and the $CHCH_2$, suggesting spin diffusion to the common site with the fastest relaxations. All the values were obtained from the slope of simple experimental decay. In the case of N(3K) at -90 °C the decay data display some tendency toward nonlinearity for the semilog plot. The results for each network are shown in Figure 16.

Mechanical and Dielectric Measurements. Dynamic mechanical storage (E′) and loss (E″) moduli at 10 Hz are shown in Figure 17 for four networks of PPO/TIPTP. The storage modulus for each sample shows a low-temperature plateau with a drop at the onset of the glass transition. The onset temperatures given in Table I are -45, -40, -15, and +30 °C for N(4K), N(2K), N(1K), and N(0.4K), respectively. These materials range from soft and pliable to hard and frangible with decreasing MW of PPO. Similarly the mechanical loss moduli go through maxima which also occur at lower temperatures with increasing molecular weight. Interestingly a low broad maximum also occurs in the loss modulus of each of the networks in the glassy region.

Dielectric loss results at 1 kHz are shown in Figure 18 for a range of temperature. Below T_g no loss is detected; N(3K), N(2K), N(1K), and N(0.4K) show respectively onset of T_g at -60, -50, -30, and +20 °C. To the low-temperature side of the T_g there is a smaller loss peak in

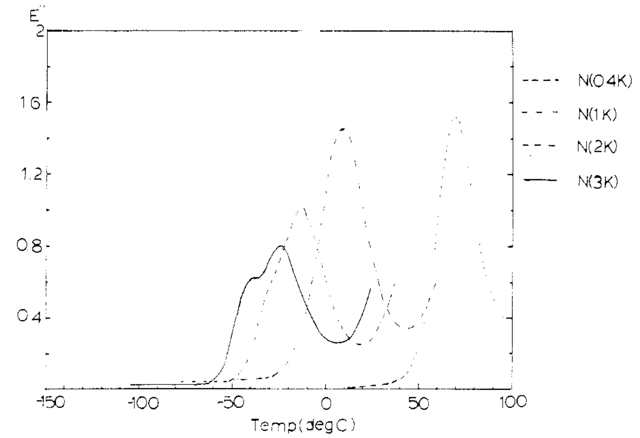

Figure 18. Variation of dielectric loss at 1 KHz with temperature for N(0.4K), - - -; N(1K), -···-, N(2K), -··-, and N(3K), —.

the N(3K) sample and a slight shoulder in the N(2K) sample: we have no understanding of their origin.

The relaxation behavior of the chain extended samples have not been determined. However, we have studied the structure-property relationship of other segmented polyether–polyurethanes by DSC.[13] Chain extension with symmetric diisocyanates yielded materials with low T_g values of −50 to −55 °C, whereas thermoplastic elastomers derived from asymmetric toluene-2,4-diisocyanate have higher T_g's of about −40 °C.

Discussion of Results

A novel objective of this motional investigation on network polymers is to explore how the cross-link influences the motion of chain segments in close proximity to it as well as those far away from it. These monomer units will be referred to as m_p and m_d where the subscripts p and d are proximal and distal, respectively. In proton NMR there is often good contact between the cross-link relaxation sites and the free-chain regions via spin diffusion. Thus T_1 data are relatively insensitive to M_c except at very high cross-link density beginning at about $M_c \approx 10m$ where m is the monomer unit molecular weight. For such materials T_1 versus temperature has a reduced slope above T_g. This is attributable to the restriction of motion due to constraints imposed by the cross-links. Rowland and Labun[7] analyzed the deviation for the single relaxation BPP theory

$$\frac{1}{T_1} = \frac{3\gamma_H^2\hbar^2}{10}\sum_j r_j^{-6}\left[\frac{\tau}{1+\omega_0^2\tau^2} + \frac{4\tau}{1+4\omega_0^2\tau^2}\right] \quad (1)$$

by treating the network T_1 as having two T_1 components corresponding to m_p and m_d

$$\frac{1}{T_1} = \frac{m_p}{T_{1p}} + \frac{m_d}{T_{1d}} \quad (2)$$

where T_{1p} and T_{1d} are the T_1 components for the proximal and distal regions with respect to the cross-links.

T_1 measurements reflect the fast motions in the megahertz region, while $T_{1\rho}$ is sensitive to the kilohertz region. Muncie et al.[8] measured $T_{1\rho}$(H) at 64 and 15 kHz to investigate the slow motions of cross-linked *cis*-polybutadiene above T_g. The results showed again insensitivity of $T_{1\rho}$(H) to M_c except for the $M_c = 14m$ sample.

Much more sensitive to the low-frequency motion is the spin–spin relaxation time. It has been shown[8,9] that T_2(H) is sensitive to long-range chain motions affected by entanglements and cross links at elevated temperatures. There was the interesting observation that T_2(H) reached a plateau in spite of the fact that the molecules are in the motional narrowing range. Several authors[14-16] have proposed a nonzero averaging of dipolar coupling due to anisotropic motions of chain segments between cross-linking modes as being responsible for this phenomenon.

These proton relaxation times are insensitive to cross-links below T_g. In a complementary way, MAS-CP-NMR seems to be ideally suited to probe molecular motions below T_g of materials which have more than one conformation in the glassy state. But, above T_g the CP sequence is ineffective and even DP experiments yield limited data. The important observations for our samples are that by CP and DP it was possible to sample regions differing in rigidity present in the network system and that relaxations of m_p and m_d can be individually discerned.

The $T_{1\rho}$(C) data of L(1K)1,4 (Figure 7) represent the simplest relaxation behavior for polymers. The values are symmetrical above and below $T_{1\rho,\min}$ which are the same for CP and DP. Jones[17] derived an expression for $T_{1\rho}$ based on the BPP theroy of relaxation due to dipolar interaction. The theory assumes an isotropic random motion of spins, a single correlation time τ_c, and an exponential decay of the correlation function for the molecular motion. However, polymers inevitably have a distribution of correlation times. These deviations are manifest in the width of the $T_{1\rho}$ minimum. Various distribution functions have been used to represent behavior of this type such as the Fuoss–Kirkwood[18] and the rectangular functions.[19] However, the relaxation data can also be fitted by a nonexponential correlation function.[20] The results of Figure 7 can be approximately fitted by a rectangular distribution function $I(\tau_c) = \tau_c^{-1} \ln (b/a)$ with $b/a \approx 10$.

The $T_{1\rho,\min}$(C) for the methyl carbons is about ten times longer than that of the backbone carbon. McCall[21] derived an approximate formula. $T_{1\rho,\min} \simeq 4\gamma B_1 T_2^2$, where T_2 is the low-temperature rigid limit transverse relaxation time, γ the gyromagnetic ratio, and B_1 is RF field strength. Therefore, T_2 for the backbone carbon resonance should be about one-third that of the methyl resonance. The actual low-temperature line-width ratio is 2:3. The predicted ($T_{1\rho}$) minima based on the low-temperature line widths of Figures 3 and 4 are more than an order of magnitude longer than the observed minima. This discrepancy indicates simply that our line widths are narrowed by MAS and decoupling and result in an artificially lengthened T_2 compared to the true rigid limit.

The values of $T_{1\rho}$(C) reach maxima at ca. −100 °C indicative of another motional process at lower temperature. The behavior resembles the T_1 data for a mixture of poly(vinyl chloride) and tetraethylene glycol dimethacrylate,[22] which displays a $T_{1,\min}$ at −165 °C for the methyl motion and a $T_{1,\max}$ at −100 °C and then decreases to a minimum for the motion of tetraethylene glycol at +10°.

Although the large changes in $T_{1\rho}$(C) below T_g do not correspond to any dramatic change in mechanical properties of the networks, we wish to note that the temperature dependence of E'' (Figure 17) below T_g shows a broad weak secondary relaxation peak for each of the networks examined. While this peak is unassigned, it appears to be correlated with the shortening of $T_{1\rho}$(C) in the same temperature region and thus from the NMR point of view, it is related to the freeing up of hindered methyl rotation in the glass.

The backbone carbon relaxation in the linear polymers is affected by the urethane linkage; there is some motional constraint for the polymer chain extended with toluene-

2,4-diisocyanate. At temperatures below $T_{1\rho,\min}$(C), the CP sequence selects for segments with reduced motion and gives $T_{1\rho}$(C) values about twice as long as those $T_{1\rho}$(C) values obtained with DP as shown in Figure 8a. On the other hand, the corresponding values for the methyl resonance are not very different (Figure 8b). In both cases the $T_{1\rho,\max}$(C) shifted to between −55 and −75 °C, which may indicate a higher temperature for the $T_{1\rho,\min}$ of methyl motion in L(1K)2,4 polymer as compared to L(1K)1,4 the polymer chain extended with phenylene-1,4-diisocyanate.

Increasing the PPO molecular weight to 3K has several consequences. The backbone motion $T_{1\rho,\min}$(C) is found at a lower temperature of ca. −45 °C as compared to the minimum at ca. −10 °C for the L(3K) polymers, in agreement with the lower T_g for the former. The $T_{1\rho}$(C) value has not reached a maximum at −90 °C, indicative of a lower temperature, $T_{1\rho,\min}$, for the methyl motion. The $T_{1\rho}$(C) values near the minimum (between −30 and −60 °C) for the methyl carbon are about 7 times greater than the backbone carbon relaxation times. The line-width data showing a narrower methyl peak are also consistent with this as showing rotational averaging of fluctuations by the methyl group.

At temperatures below the $T_{1\rho,\min}$, the decay of the backbone carbon magnetization in the rotating frame for the network polymers is biphasic except in the N(3K) case. This is in contrast to the methyl carbon resonances of all the network systems, all of which decay as a single exponential. It seems that the PPO chains with M_c from 0.4K to 2K are characterized by two regions that interact differently with the lattice.

The earliest demonstrated examples of relaxation heterogeneity are the semicrystalline polymers. However, if the two regions are partially coupled via spin diffusion, then it is possible for the amorphous component that is tightly coupled to the lattice to relax the nuclei in the crystalline component which is weakly coupled to the lattice. Thus, only a single T_1(H) is observed at −20 °C for polyethylene.[23] Many glassy polymers have been found to show a distribution of relaxation times for each type of carbon.[24,25]

The short $T_{1\rho}$ component of the N(1K) and N(2K) backbone carbons have nearly the same relaxation times as the aromatic carbon resonance. In the case of the N(0.4K) sample the $T_{1\rho}$ (backbone C) versus temperature parallels that of the aromatic carbon resonance; the relaxation time values are about the same at 1–2 ms over a broad range in the vicinity of minimum but are somewhat longer for the backbone carbon of PPO. The observation over such a broad temperature range of short $T_{1\rho}$(C) values for the methyl, backbone, and aromatic resonances is characteristic of the networks especially in comparison to the relatively narrow minima seen for the linear polymers. The molecular cause of this broad region of short $T_{1\rho}$(C) cannot as yet be unambiguously assigned. Both phenyl motion and methyl motion are reasonable candidates. In domains near the cross-links the phenyl group proximity and concentration make them plausible contributors to $T_{1\rho}$, but if the methyl group rotation is restricted by the packing in the cross-linked region, they too could contribute to $T_{1\rho}$(C) as they overcome the barrier restrictions with increasing temperature. The further observation that the $T_{1\rho}$(H) values are similarly short indicates that either the ^{1}H or ^{13}C is somewhat coupled during the spin lock decay period and/or both are affected by similar processes. Domains distant from the cross-link would then be assigned to the longer relaxation component. As M_c is increased the effect of cross-links is diluted out so that $T_{1\rho}$(C) of N(3K) resembles that of L(3K). Undoubtedly spin diffusion plays a role in the observed relaxation times but that is not as yet experimentally accessible. Also, as direct dipolar relaxation of carbons can occur in competition with motional relaxation, their relative importance is not as yet resolved. ADRF experiments are underway to resolve this question.

In the case of heterogeneity in T_2 relaxation, one can estimate the fractions of nuclei with different relaxation rates. But both the magnitude and intensity of the $T_{1\rho}$ decay may be affected by spin diffusion, and the component intensities of such coupled systems bear no direct relationship on the number of resonant nuclei contributing to the individual decay terms.[26] The values of short $T_{1\rho}$ were those of the initial decay slope. The error is large when one attempts to subtract the slow decay component from the fast one.

This study also shows that $T_{1\rho}$(C) by CP is not a reliable method to determine T_g in networks. There is no minimum for the N(0.4K) sample in Figure 11. There are also no $T_{1\rho,\min}$ for either the backbone or the methyl carbon by CP for the N(1K) sample (Figure 12). Distinct $T_{1\rho,\min}$ were obtained by DP, but the minimum was found at ca. 0°, which is considerably higher than the T_g obtained by the other methods. Sharp $T_{1\rho}$ minima were found at −30 °C by both CP and DP for the N(3K) system; the T_g value is −40 and −60 °C according to the dynamic mechanical and dielectric measurements, respectively. It appears that the sensitivity of NMR to local and small motions makes the T_g measured by NMR problematically related to T_g by more mechanical methods.

The relaxation data for NMR-$T_{1\rho}$(C), DETA, and DMTA for N(1K) show maxima ($\omega = 1$) at approximately 0, +10, and −5 °C. On the basis of observing frequency one calculates $\tau_c = 10^{-5}$, 10^{-3}, and 10^{-1} s, respectively, at these temperatures. The range of these correlation times points out the large differences as to what each technique measures even though they are all interpreted by the same power spectrum formalism. DMTA measures the whole complex of intermolecular interactions that contribute to bulk modulus. DETA is limited to detecting the mobility of the electric dipole of the C–O–C bonds in the backbone. NMR relaxation is sensitive to all motions that modulate the magnetic dipolar interactions, including backbone segments, methyl rotations, and phenyl group motion. In no way are the correlation times expected to be the same. That the NMR correlation time is several orders of magnitude shorter than that for DMTA reflects the occurrence of magnetic dipolar/motional events which are of low energy and are not reflected in the macroscopic modulus.

A considerable amount of further work on several series of network systems will be necessary in order to separate contributions to the NMR relaxation and to interrelate relaxation techniques.

Conclusions

The spin–lattice relaxation of ^{13}C nuclei has been shown to be sensitive to cross-links below T_g whereas the spin–spin relaxation is insensitive in this temperature regime. A distribution of correlation times is demonstrated for network systems with short segmental lengths between cross-links. The short relaxation component has been attributed to the backbone carbon in close proximity to the cross-link. This has yet to be proven by study by selective ^{13}C enrichment of the terminal carbons in the α,ω-dihydroxypoly(propylene oxide). The close coupling of the proximal carbon atoms with the phenyl group of TIPTP may be influenced by its very large molecular size of this junction molecule. Networks with PPO directly cross-linked to phosphorus atoms will be studied in order to better approximate point cross-links.

Acknowledgment. This work was supported in part by the Materials Research Laboratory of the University of Massachusetts.

Registry No. (PO)(TIPTP) (copolymer), 111769-80-3; (PO)(phenylene-1,4-diisocyanate) (copolymer), 111743-18-1; (PO)(toluene-2,4-diisocyanate) (copolymer), 31370-60-2.

References and Notes

(1) Slichter, W. P. *Rubber Chem. Technol.* **1961**, *34*, 1574.
(2) Slichter, W. P.; Davis, D. D. *J. Appl. Phys.* **1964**, *35*, 3103.
(3) McCall, D. W.; Douglass, D. C. *Appl. Phys. Lett.* **1965**, *7*, 12.
(4) Connor, T. M.; Hartland, A. *Polymer* **1968**, *9*, 591.
(5) McBrierty, V. J.; Douglass, D. C. *Macromol. Rev.* **1981**, *16*, 95.
(6) McBrierty, V. J. *Magn. Reson. Rev.* **1983**, *8*, 165.
(7) Rowland, T. J.; Labun, L. C. *Macromolecules* **1978**, *11*, 466.
(8) Muncie, G. C.; Jonas, J.; Rowland, T. J. *J. Polym. Sci., Polym. Chem. Ed.* **1980**, *18*, 1061.
(9) (a) Folland, R.; Charlesby, A. *Polymer* **1979**, *20*, 207. (b) Folland, R.; Charlesby, A. *Polymer* **1979**, *20*, 211.
(10) Charlesby, A.; Folland, R.; Steven, J. H. *Proc. R. Soc. London, Ser. A* **1977**, *355*, 189.
(11) Schaefer, J. *Macromolecules* **1973**, *6*, 882.
(12) Schaefer, J.; Chin, S. H.; Weissman, S. I. *Macromolecules* **1972**, *5*, 798.
(13) Woo, E. J.; Farber, G.; Farris, R. J.; Lillya, C. P., Chien, J. C. W. *Polym. Eng. Sci.* **1985**, *25*, 834.
(14) McCall, D. W., Douglass, D. C., Anderson, E. W. *J. Polym. Sci.* **1962**, *59*, 301.
(15) (a) Charlesby, A.; Folland, R.; Steven, J. H. *Proc. R. Soc. London, Ser. A* **1977**, *355*, 189. (b) Folland, R.; Steven, J. H.; Charlesby, A. *J. Polym. Sci.* **1978**, *16*, 1041.
(16) (a) Cohen-Addad, J. P. *J. Chem. Phys.* **1974**, *60*, 2940. (b) *J. Chem. Phys.* **1975**, *63*, 4880.
(17) Gotlib, Yu. Ya.; Lifshits, M. I.; Shevelev, V. A.; Lishansii, V. A.; Balanina, I. V. *Vysokomol. Soedin, Ser. A* **1976**, *18*, 2299.
(18) Jones, G. P. *Phys. Rev.* **1966**, *148*, 332.
(19) Fuoss, R. M.; Kirkwood, J. G. *J. Am. Chem. Soc.* **1941**, *63*, 385.
(20) McCall, D. W.; Douglass, D. C.; Anderson, E. W. *J. Chem. Phys.* **1959**, *30*, 1272.
(21) Connor, T. M. *J. Polym. Sci., Polym. Phys. Ed.* **1970**, *8*, 191.
(22) McCall, D. W. *Acc. Chem. Res.* **1971**, *4*, 223.
(23) Davis, D. D.; Slichter, W. P. *Macromolecules* **1973**; *6*, 728.
(24) Crist, B.; Peterlin, A. *J. Polym. Sci., Polym. Phys. Ed.* **1969**, *7*, 1165.
(25) Schaefer, J.; Stejskal, E. O.; Buchdahl, R. *Macromolecules* **1977**, *10*, 384.
(26) Schaefer, J.; Stejskal, E. O.; Buchdahl, R. *Macromolecules* **1974**, *8*, 291.
(27) Woessner, D. E. *J. Chem. Phys.* **1962**, *34*, 41.

Hydrogen Bonding in Polymer Blends. 3. Blends Involving Polymers Containing Methacrylic Acid and Ether Groups

Joon Y. Lee, Paul C. Painter, and Michael M. Coleman*

Department of Materials Science and Engineering, The Pennsylvania State University, University Park, Pennsylvania 16802. *Received May 11, 1987*

ABSTRACT: Poly(ethylene-*co*-methacrylic acid) (EMAA) copolymers are strongly self-associated in the condensed state at ambient temperatures through the formation of intermolecular carboxylic acid dimers. Polyethers, in contrast, are polymers that are inherently weakly self-associated but associate strongly with EMAA by forming intermolecular hydrogen bonds between the carboxylic acid and ether oxygen groups. In this paper we present the results of Fourier transform infrared studies of EMAA copolymer blends containing poly(vinyl methyl ether) and ethylene oxide-*co*-propylene oxide copolymers. The blends studied were found to be extensively mixed at the molecular level in the amorphous state. Quantitative measurements of the fraction of EMAA carboxylic acid groups that are hydrogen bonded to ether groups have been obtained in blends of different compositions, and the results are discussed in terms of competing equilibria.

Introduction

During the past 10 years we have taken advantage of the unique sensitivity of FTIR spectroscopy to specific types of intermolecular interactions (most notably hydrogen bonds) in order to probe the molecular structure of multicomponent polymer systems, especially polymer blends. Much of this work has been summarized in a recent review.[1] More recently, we have employed conventional transmission FTIR spectroscopy to obtain a measure of the relative strength and concentration of intermolecular interactions (hydrogen bonds) in strongly self-associated polymers such as polyamides[2-4] and polyurethanes.[5] This led to studies of miscible, or partially miscible, polymer mixtures containing such polymers[6,7] and to a simple model of specific, directional interactions based upon an equilibrium theory.[8,9]

In our search for miscible or partially miscible binary polymer blends containing a strongly self-associated polymer, we have used the following simple axiom. Significant mixing at the molecular level is most likely to occur with a weakly self-associated polymer capable of forming a favorable interaction with it. In this vein, we have published the results of studies performed on amorphous polyamide–poly(2-vinyl pyridine) (P2VP)[6] and amorphous polyurethane–poly(ethylene oxide-*co*-propylene oxide) (EPO)[7] blends, both of which exhibit a high degree of molecular mixing. Here we report on our studies of a series of polymer blends in which one of the components is a polymer containing methacrylic acid (MAA) units. Unlike polyamides and polyurethanes that form a distribution of "chains" of hydrogen-bonded amide and urethane groups in the condensed state,[7,9] MAA containing polymers are strongly self-associated at ambient temperatures through characteristic intermolecular hydrogen-bonded dimers. Our guiding principles are the same, however, and significant molecular mixing of MAA polymers can be achieved with other polymers containing ether units.

Experimental Section

Ethylene–methacrylic acid copolymers (EMAA) were synthesized in the laboratories of the E. I. Du Pont de Nemours Co. Four different copolymers containing 18, 32, 44, and 55 wt % MAA (denoted EMAA[18], EMAA[32], etc.) were used in our studies.

0024-9297/88/2221-0346$01.50/0 © 1988 American Chemical Society